
Figure S1. Longitudinal Sampling Overcomes Heterogeneity Seen across Cross-Sectional Microbiome Studies, Related to Figure 1

(A) Cohort description. Age in years.

(B) Dotplot of the number of taxa and metabolites identified at $FDR < 0.25$ for the comparisons in the 3 panels (Two-sided Mann-Whitney U -test). For the metagenomics panels on the left selected groups of taxa names are listed to illustrate that there is no overlap between taxa that are identified in data from one of the time points (0-6) and the collapsed data. Colors indicate different taxonomic levels. For the metabolomics panel on the right names for all metabolites that met the threshold are indicated. There is a higher level of cross-sectional consistency in the metabolome compared to the microbiome (for n numbers see [Table S1](#)). (C) Representative plots displaying the relative abundance of 4 *Streptococcus* sp. that are found at significantly higher abundances in IBS compared to HC ($n = 51$, 24 averaged gut microbiome profiles for IBS and HC, respectively). Two-sided Mann-Whitney U -test $FDR < 0.25$ (results from all comparisons can be found in [Table S2](#)).

(D) Representative plots displaying the relative abundance of 2 phyla that are significantly depleted in IBS-D compared to HC ($n = 29$, 24 averaged gut microbiome profiles for IBS-D and HC, respectively). Two-sided Mann-Whitney U -test $FDR < 0.25$.

(E) Representative plots displaying the relative abundance of 2 species that are significantly elevated in IBS-C compared to HC ($n = 22$, 24 averaged gut microbiome profiles for IBS-C and HC, respectively). Two-sided Mann-Whitney U -test $FDR < 0.25$.

(F) Representative plots displaying the relative abundance of 2 bacterial families that are found at significantly higher abundances in IBS compared to HC ($n = 51$, 24 averaged gut microbiome profiles for IBS and HC, respectively). Two-sided Mann-Whitney U -test $FDR < 0.25$.

(G) Representative plots showing abundance of Proteobacteria in colonic biopsies obtained from IBS-C and HC at two different time points (T1; $n = 29$, 13 and T2; $n = 21$, 9 averaged gut microbiome profiles for IBS and HC, respectively). Two-sided Mann-Whitney U -test $FDR < 0.25$.

Boxplot center represents median and box interquartile range (IQR). Whiskers extend to most extreme data point $< 1.5 \times IQR$.

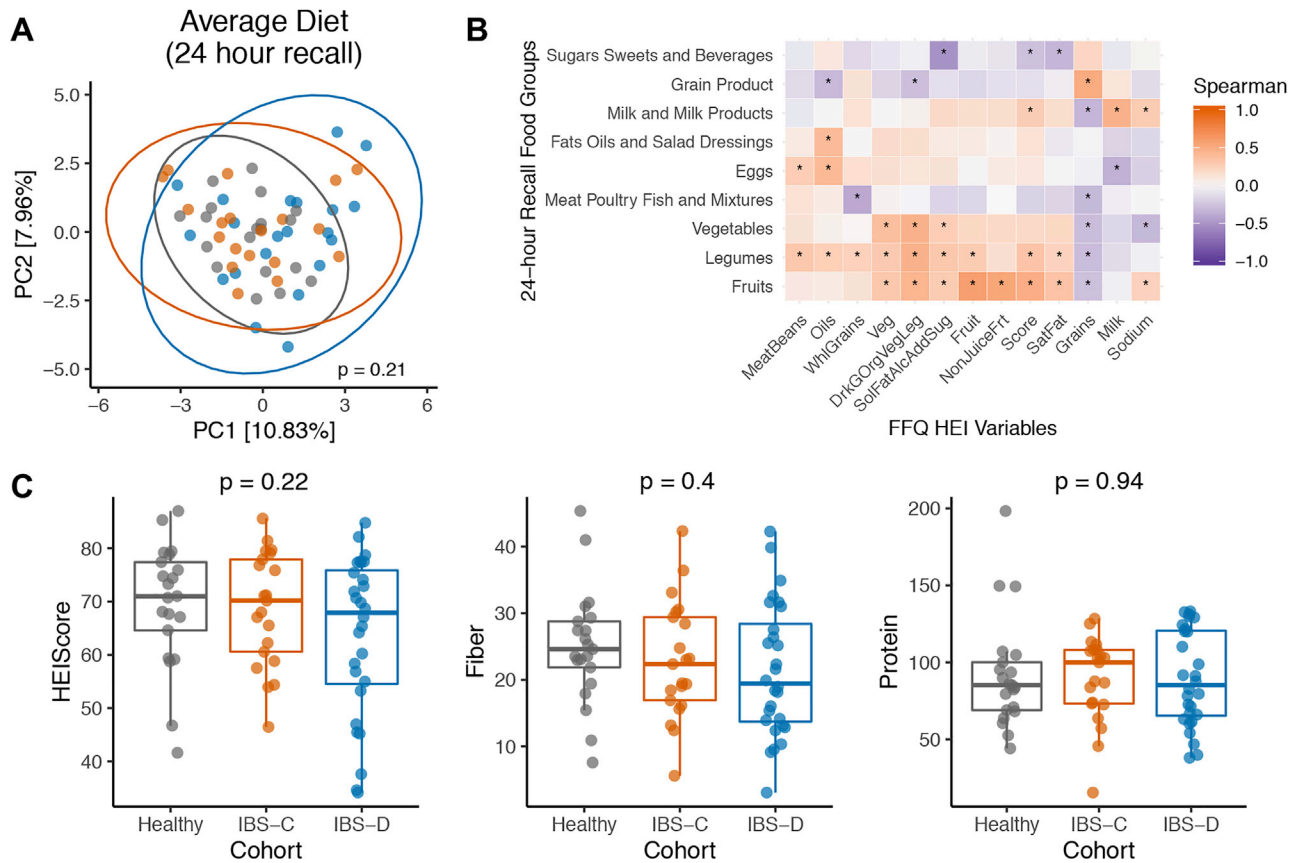


Figure S2. No Differences in Dietary Intake between Cohorts, Related to Figure 1

(A) Average food intake from 24-hour recalls was assessed using tree-based food diversity analysis. Dietary diversity was not different between cohorts (PERMANOVA, $p = 0.21$, 999 permutations).

(B) Dietary intake data from 24-hour recalls shared similarities with baseline food frequency questionnaires (FFQ) and 24-hour recall food groups were correlated with FFQ measured Healthy Eating Index (HEI) scores and variables (Spearman correlation, * indicates FDR corrected p value < 0.25).

(C) FFQ measured HEI Scores, fiber intake, and protein intake were not different between cohorts.

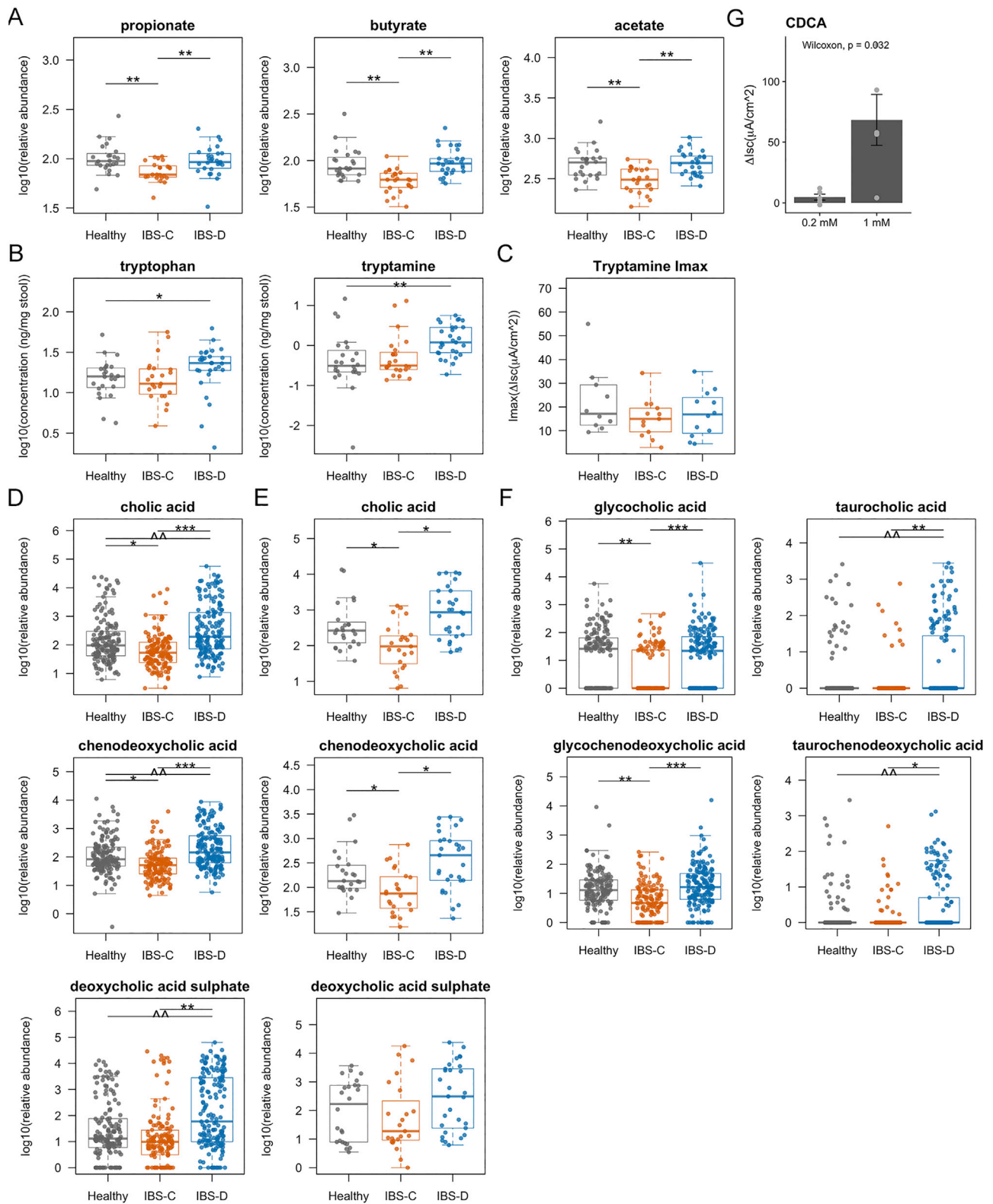


Figure S3. Averaged Metabolomics Data and Additional Physiologic Measurements, Related to Figure 2

(A) Relative abundance of propionate, butyrate, and acetate in stool samples determined with ¹H NMR (averaged data per subject, FDR adjusted pairwise Mann-Whitney tests, $n = 23, 29, 24$ averaged metabolomes for IBS-C, IBS-D, and HC, respectively).

(legend continued on next page)

(B) Absolute abundance of tryptophan and tryptamine in a subset of the stool samples determined with LC-MS/MS (ng/mg stool) (averaged data per subject, FDR adjusted pairwise Two-sided Mann-Whitney *U*-test, $n = 23, 29, 24$ averaged metabolomes for IBS-C, IBS-D, and HC, respectively).

(C) Maximal ΔI_{sc} (I_{max}) following application of increasing concentrations of tryptamine basolaterally in colonic biopsies from time-point 1 (no significant difference ANOVA Tukey, $n = 13, 12, 10$ colonic biopsies for IBS-C, IBS-D, and HC, respectively).

(D) Relative abundance of bile acids cholic acid, chenodeoxycholic acid, and deoxycholic acid sulfate in stool samples determined with LC-MS/MS (linear mixed-effect models on log₁₀-transformed data correcting for subject, FDR adjusted, $n = 136, 170, 146$ metabolite profiles for IBS-C, IBS-D, and HC, respectively).

(E) Relative abundance of bile acids cholic acid, chenodeoxycholic acid, and deoxycholic acid sulfate in stool samples determined with LC-MS/MS (averaged data per subject, FDR adjusted pairwise Two-sided Mann-Whitney *U*-test, $n = 23, 29, 24$ averaged metabolomes for IBS-C, IBS-D, and HC, respectively).

(F) Relative abundance of bile acids glycocholic acid, taurocholic acid, glycochenodeoxycholic acid, and taurochenodeoxycholic acid in stool samples determined with LC-MS/MS (linear mixed-effect models on log₁₀-transformed data correcting for subject, FDR adjusted, $n = 136, 170, 146$ metabolite profiles for IBS-C, IBS-D, and HC, respectively).

(G) ΔI_{sc} (I_{max}) following application CDCA basolaterally in proximal colon mucosa submucosa preparations from germ free mice ($n = 3$ mice, Wilcoxon signed rank test, error bars indicate SE).

Boxplot center represents median and box interquartile range (IQR). Whiskers extend to most extreme data point $< 1.5 \times$ IQR. Symbols indicate significance (** < 0.001 , ** < 0.01 , * < 0.05 , ^ < 0.1 , ^ < 0.2).

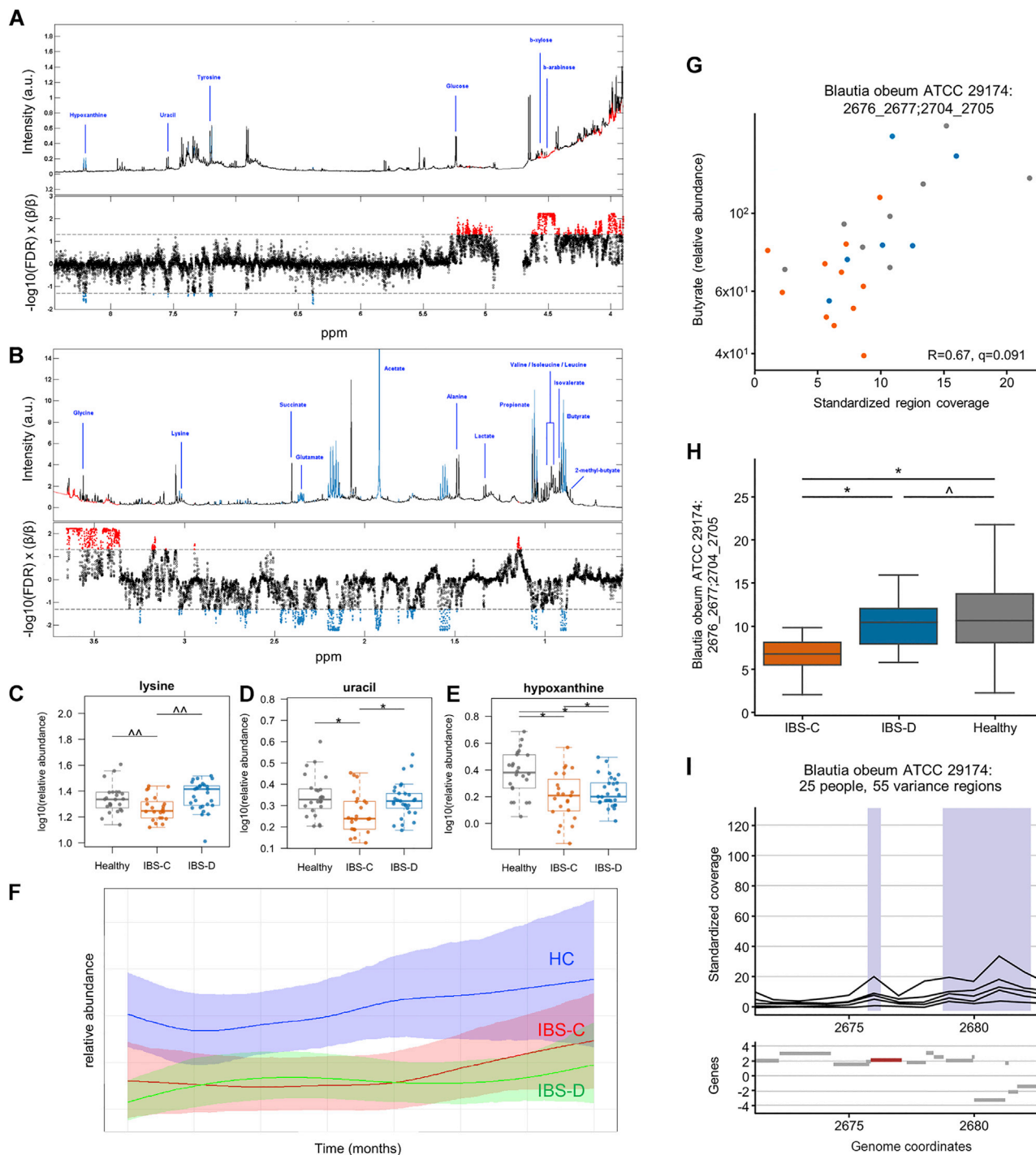


Figure S4. Averaged and Additional Metabolomics and Integration Data, Related to Figures 3 and 4

(A) Projection-to-latent-structures-discriminant-analysis (PLS-DA) results shown for the 3.8 - 8.5 ppm range of the 600 MHz ^1H NMR spectrum for IBS-C stool samples compared to healthy control samples. Top panels display the averaged spectra with blue features representing features that the model identifies to have a lower relative abundance in IBS-C compare to HC. Bottom panel shows the corresponding Manhattan plot for all 30611 spectral variables in the OPLS-DA model. Variables in red indicate higher relative abundance. However, these variables correspond to noise and have no metabolite feature assigned. PLS-DA model characteristics were $R^2Y = 0.28$, $Q^2Y = 0.15$, $RCV = 0.88$ ($n = 136, 146$ metabolite profiles for IBS-C and HC, respectively)

(B) Same as panel A for spectral range of 0 -3.8 ppm

(C) Relative abundance of lysine in stool samples determined with ^1H NMR (FDR adjusted pairwise Two-sided Mann-Whitney U -test, ($n = 23, 29, 24$ averaged metabolomes for IBS-C, IBS-D, and HC, respectively).

(legend continued on next page)

(D) Relative abundance of uracil in stool samples determined with ^1H NMR.

(E) Relative abundance of hypoxanthine in stool samples determined with ^1H NMR.

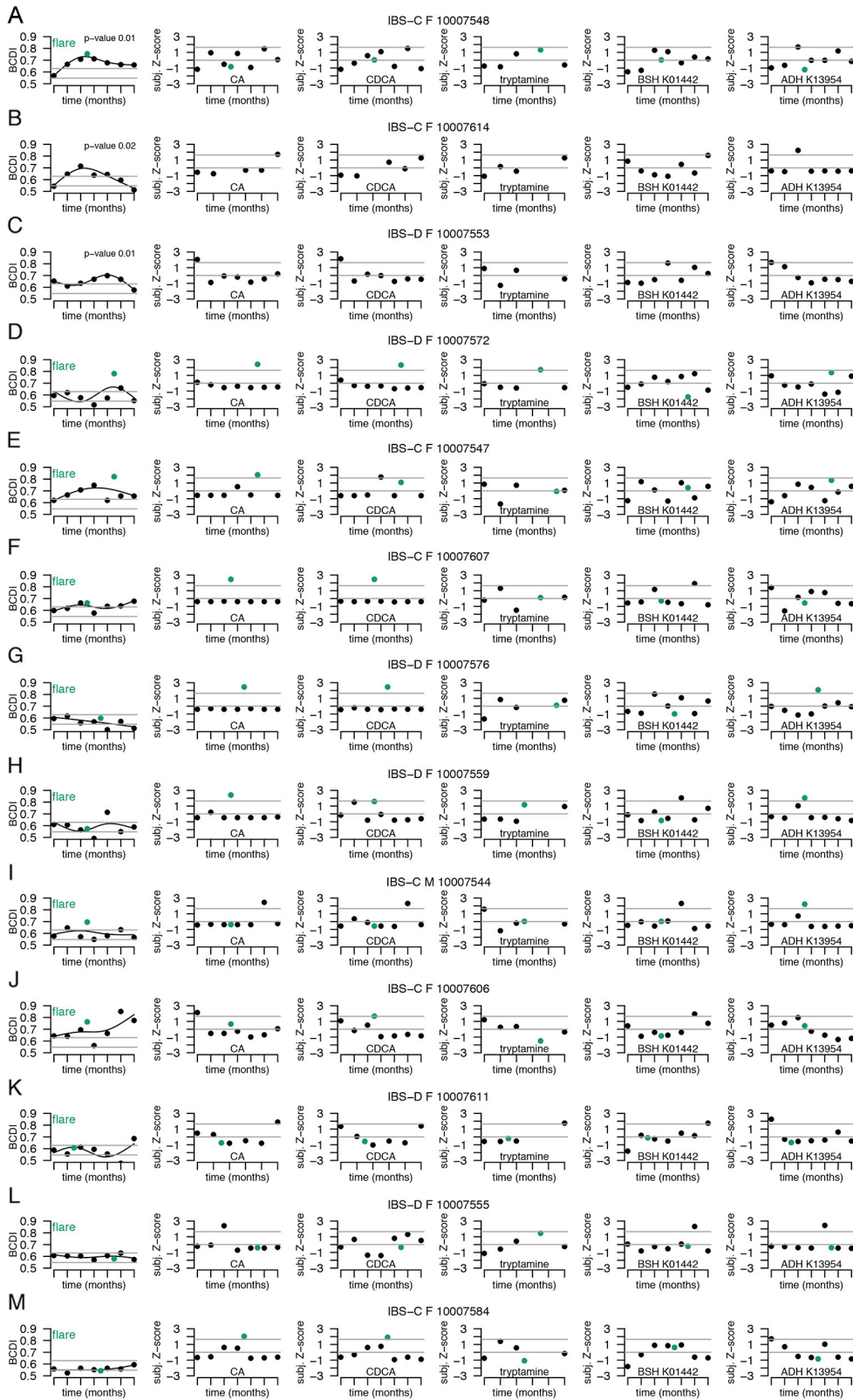
(F) Time course analysis using santaR for hypoxanthine showing hypoxanthine is consistently lower in IBS-C and IBS-D. The analysis is based on 1,000 bootstrap rounds (95% confidence interval), 1,000 permutation rounds and 4 degrees of freedom.

(G) Scatterplot of metabolite intensities and standardized region coverage for SV association result for *Blautia obeum* ATCC 29 genomic regions positively correlated to butyrate (Spearman correlation inset, $n = 11, 6, 8$ averaged microbiome abundances with *Blautia obeum* ATCC 29 present above threshold for IBS-C, IBS-D, and HC, respectively).

(H) Mann-Whitney U -test comparison of genomic region abundance from G across cohorts.

(I) Genomic context of region from G with relevant gene highlighted in red.

Boxplot center represents median and box interquartile range (IQR). Whiskers extend to most extreme data point $< 1.5 \times \text{IQR}$. Symbols indicate significance (** < 0.001 , ** < 0.01 , * < 0.05 , $\wedge < 0.1$, $\wedge < 0.2$).



(legend on next page)

Figure S5. Alteration in Gut Microbiome and Microbial Metabolites Underlie Flares in IBS Patients, Related to Figure 5

(A-M) The same 6 features are plotted for 13 subjects in panels A-M. The most left plot (1st column) represents the Bray-Curtis dissimilarity (BCD)-based irregularity for microbiome stool samples. Significant time-dependent patterns are indicated with a p value (p value from sum of squares of 3rd order polynomial fits from 99 perturbations). Black line is a 3rd order polynomial spline fit. Grey lines indicate median and 90th percentile of median HC dissimilarities, green dots indicate a flare. For the other plots the personalized Z-scores of the indicated metabolites (2nd – 4th column) and KEGG modules (5th and 6th column) are plotted. In these plots gray horizontal lines indicate the Z-score at 0 and at alpha level of 0.05 ($|Z| = 1.645$). Green dots again indicate flare samples.

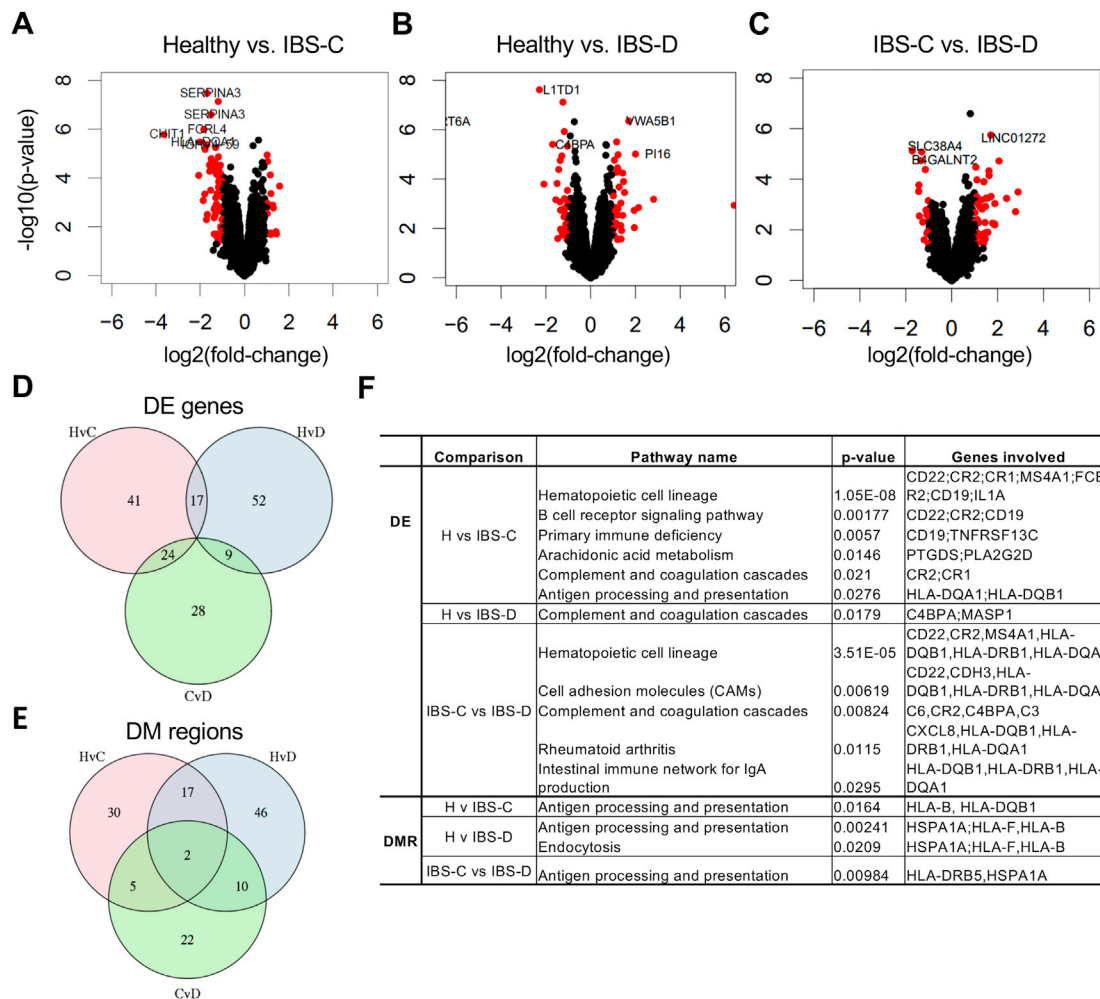


Figure S6. Epigenetic and Transcriptomic Changes in Colonic Biopsies as a Measure of Host Physiologic State in IBS, Related to Figure 7 (A) Volcano plot of differentially expressed (DE) genes when comparing HC and IBS-C from T1 samples. Genes with absolute log₂ fold change ≥ 1 and nominal p value < 0.05 are colored in red (generalized binomial test from edgeR, n = 14, 6, 8 time point 1 biopsy transcriptomes from female IBS-C, IBS-D, and HC subjects, respectively).

(B) Same as in A for HC and IBS-D comparison.

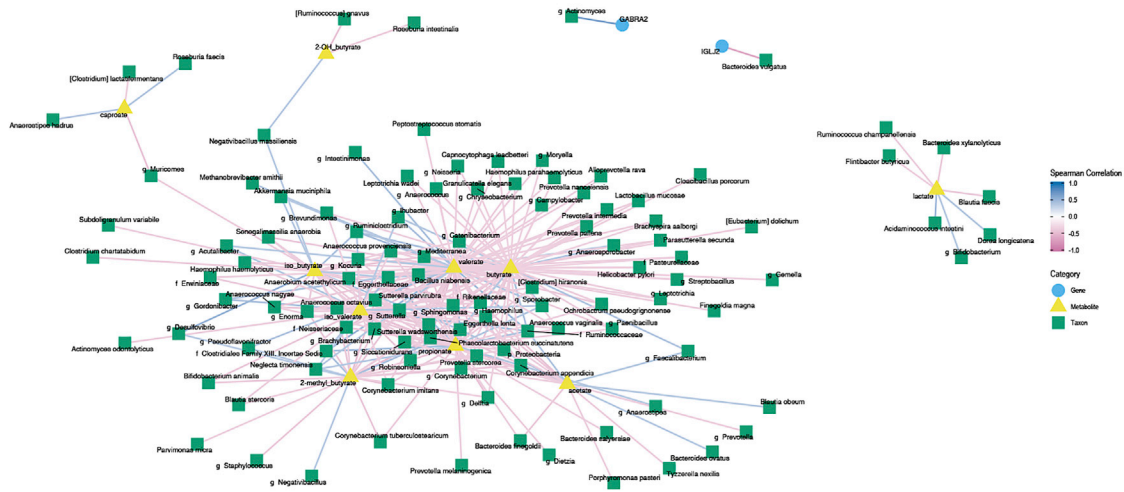
(C) Same as in A for the IBS-C and IBS-D comparison.

(D) Venn diagram displaying the number of genes that overlap between significantly DE genes from HC versus IBS-C comparison (HvC), HC versus IBS-D comparison (HvD), and IBS-C and IBS-D comparison (CvD).

(E) Venn diagram displaying the number of genes that overlap between significant differentially methylated regions (DMR) from HC versus IBS-C comparison (HvC), HC versus IBS-D comparison (HvD), and IBS-C and IBS-D comparison (CvD) (Clusters of differentially methylated CpGs (p value < 0.01 and > 5% difference in methylation) identified with bump hunter algorithm defined as a minimum of 4 probes in the region with adjusted DMR p value < 0.05 through permutation test, n = 14, 6, 8 time point 1 biopsy methylome profiles from female IBS-C, IBS-D, and HC subjects, respectively).

(F) KEGG pathway enrichment results for significant DE and DMR genes (see above for definitions of DE and DMR; p value < 0.05 from RITAN KEGG enrichment).

A Biopsy at T1 (FDR adjusted $p < 0.3$)



B Luminal (FDR adjusted $p < 0.25$)

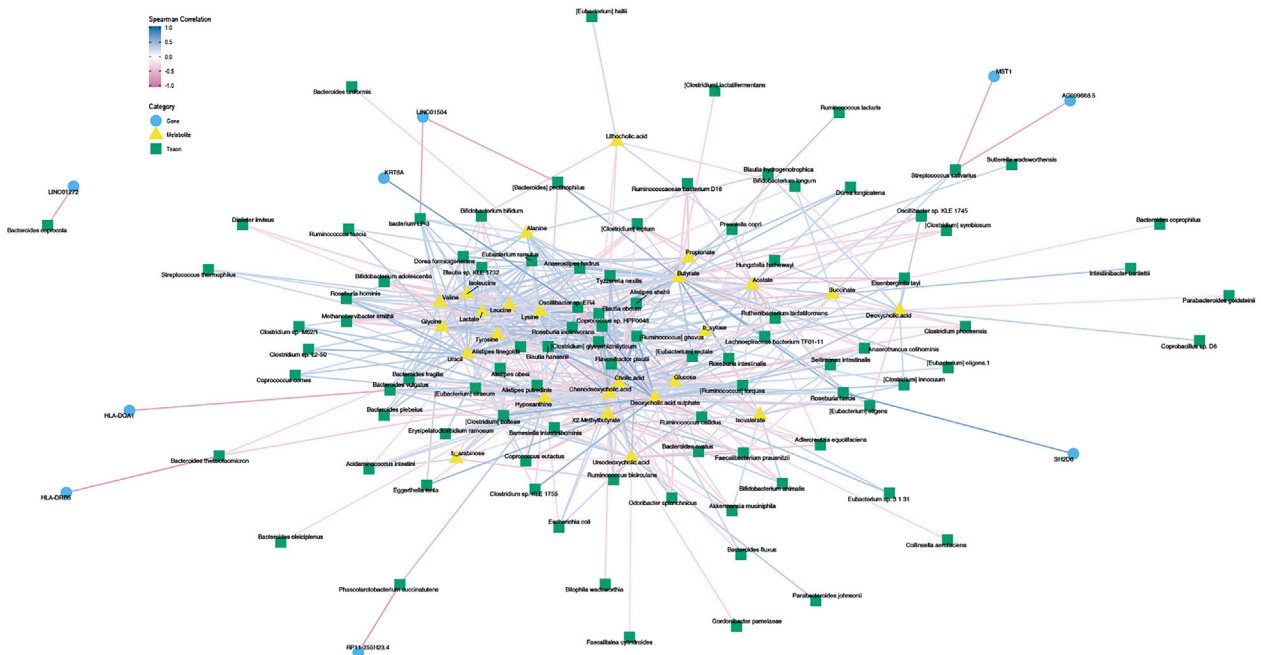


Figure S7. Data Integration Using Correlation Networks, Related to Figure 6

(A) Biopsy Spearman correlation network containing time point 1 host transcriptome, biopsy metabolome and biopsy microbiome.
 (B) Luminal Spearman correlation network containing collapsed host transcriptome, luminal metabolome and luminal microbiome.